01 Sep 2011

Electron Transport Through Two Irreducibly-Coupled Aharonov-Bohm Rings with Applications to Nanostructure Quantum Computing Circuits

C. A. Cain

Cheng-Hsiao Wu
Missouri University of Science and Technology, chw@mst.edu

Recommended Citation

C. A. Cain and C. Wu, "Electron Transport Through Two Irreducibly-Coupled Aharonov-Bohm Rings with Applications to Nanostructure Quantum Computing Circuits," *Journal of Applied Physics*, vol. 110, no. 5, American Institute of Physics (AIP), Sep 2011.
The definitive version is available at https://doi.org/10.1063/1.3631782

Electron transport through two irreducibly-coupled Aharonov-Bohm rings with applications to nanostructure quantum computing circuits

C. A. Cain and C. H. Wu[a)]
Department of Electrical and Computer Engineering, Missouri University of Science and Technology, 301 W 16th St, Rolla, Missouri 65409, USA

(Received 16 February 2011; accepted 31 July 2011; published online 12 September 2011)

We investigated several classes of two coupled Aharonov-Bohm rings that share a finite center common path, where the phase of the electron wave function can be modulated by two distinct magnetic fluxes. The coupling is similar to two coupled atoms. The behavior of charge accumulation along the center common path or, equivalently, the bonding and anti-bonding of the two rings can be achieved as the two applied fluxes are varied. Thus, when three external terminals are connected to such coupled rings, the behavior of the electron transport is divided into several classes, depending on the number of atoms in each ring and the locations of the terminals. The results are presented here. The applicable electron wave computing circuits are discussed. In particular, a half-adder construction is shown here by employing the symmetric and anti-symmetric properties of the transmission of a given terminal when the sign of the flux is changed. The analogy of two coupled rings with respect to two spins allows one to make a further connection with traditional spintronics-based schemes. © *2011 American Institute of Physics*. [doi:10.1063/1.3631782]

I. INTRODUCTION

The Aharonov-Bohm (AB) effect has been well studied.[1–8] An AB ring can be considered as a man-made atom. The clockwise (counter-clockwise) circulation of the persistent current can also have an analogy with the spin-up (spin-down) of spin-based electronics.[9] The electron density in an isolated ring can be considered as uniform throughout the entire ring in a uniform positive background of ionic charge of a metal. The flux periodicity is thus an elementary flux quantum $\Phi_0 = hc/e$. When two external terminals are connected to such an isolated AB ring, the electron transport from one terminal to the other exhibits several different classes of behavior in a strictly one-dimensional ballistic model.[10] Thicker small-scale coupled AB rings have also been investigated.[11] This is similar to microwave propagation in a waveguide. The fundamental modes in microwaves are classified by the waveguide's geometrical properties, such as the aspect ratio of the cross section in the rectangular case. However, in a two-terminal AB ring, as an electron waveguide, the transmission behavior is classified by the total number of atoms, or nodes, on the one-dimensional ring and the relative locations of the two terminals. Even-numbered and odd-numbered rings form two different classes of transport. In particular, for an odd-numbered AB ring, the distance between the two terminals, as measured from the upper and lower paths of the ring, must differ by at least one atomic spacing. This results in a universal double flux periodicity $(\Phi_0/_2)$ for the odd-numbered rings, while even-numbered rings will have a single flux periodicity Φ_0. Larger one-dimensional rings are similar to their smaller counterparts, since scaling laws exist to preserve the transmission behavior if the ring size is scaled up an even or odd number of times, as long as the electron coherence is maintained.[10,12,13]

When two or more AB rings are interacting together by an added bound length, or path between the two rings, the flux periodicity is unchanged. This is a property of reducible networks, because each ring can be modulated by one flux only. However, in an irreducible network, when two AB rings are merged to form an interacting center common path (as shown in Fig. 1), there is a charge transfer from other locations of the ring to the center common path to form a bonding or anti-bonding orbital.[14] In this case, the phase of an electron wave function on this center common path can now be modulated by the two applied fluxes on either side. This is similar to the situation when two atoms are brought together to form a molecule. However, this bonding and anti-bonding behavior, or the charge transfer into or out of the center common path, can be manipulated by controlling the two applied fluxes. Thus, this space charge effect, or capacitance effect,[8] is not limited to a p-n junction from two different semiconductor types. In nanoscale metals, this pure semiconductor equilibrium charge transfer behavior can be seen in metallic rings.[14] This points out that the transport of an electron in electron waveguides is both resistive (elastic scattering at the nodes) and capacitive (due to the space charge), just like electron transport through a classical diode.

In this paper, we investigated the electron transport through two irreducible AB rings (Fig. 1). This is motivated by the possibility of using such quantum networks for computing circuits. Earlier effort in this area by one of us[12,13] centered on a single AB ring having three or four external terminals. Multi-terminal AB rings can then be used for computing by employing two or three coherent inputs. Thus, logic gates and full/half-adders are constructed based on the vector sum of these inputs. However, spintronics-based computing uses different inputs.[9] If the spin-up (spin-down) concept is

[a)]Author to whom correspondence should be addressed. Electronic mail: chw@mst.edu.

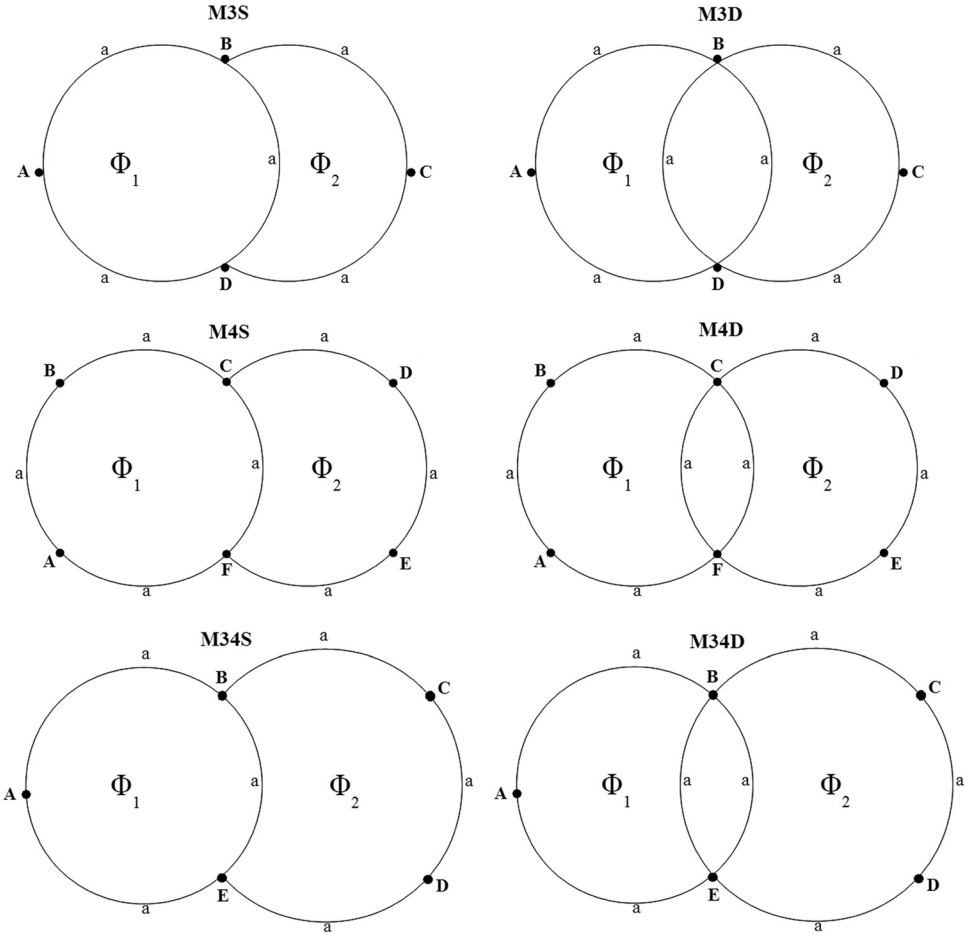

FIG. 1. The six irreducibly coupled AB ring network configurations. Dots are the location of atoms with spacing a to the nearest neighbors. In the double-bond figures, the two center paths are closely spaced together, but drawn apart for clarity purposes. In the single-bond figures, the center common path is drawn distorted. The two rings have the same flux area.

associated with an AB ring having clockwise (counter-clockwise) circulation of the persistent current, then it is possible to construct the four rules of a half-adder using the four configurations of spin pairings (or AB ring pairings), even though the coupling of spins and of AB rings are different. But note that, in coupled AB rings, the entanglement is guaranteed as long as the coherence length is larger than the entire network.

In Sec. II, we present the quantum network model of the irreducible network for two coupled AB rings. This is formulated through the node-equation approach developed by one of us earlier.[10,12,13] In this approach, a simple AB ring can be considered as a ring of harmonic oscillators, except now the applied fluxes can further modulate the phase of the oscillators. The equivalence of our node equation approach, with respect to traditional scattering matrix methods, has been established.[10] The band structure and persistent current for the three different classes of irreducibly coupled AB rings are described first, with a detailed example given for a particular even-even combination. When the center common path is modulated by two different fluxes, Φ_1 and Φ_2 (as shown in Fig. 1), the Brillouin zone is two-dimensional. Thus, the flux periodicity is always a rational number. Note that the presence of a tunneling path in a simple AB ring can also be modeled as having a center common path.[15] In Sec. III, we describe the node equation approach when the isolated coupled rings are further perturbed by attaching multiple external terminals. The number of external terminals is chosen to be three for good reason. If the number is only two, the constructed one-dimensional chain of irreducible networks can only further narrow down the transmission range. This has been investigated earlier[14] and limits the possible logic applications. For four or more terminals, the transmission probabilities will be distributed to all terminals and is then useless for constructing a computing circuit because logical outputs cannot be distinctively determined any longer. As we will show, only in a three-terminal situation can an input still be transferred totally to one of the two output terminals. Additionally, the three primary classes of transmission behavior observable in two irreducibly coupled AB rings having three terminals are presented. They represent the fundamental modes of propagation, just like microwave propagation in classical waveguides. In Sec. IV, we show a class of propagation that may be useful for constructing a half-adder circuit. When two binary digits are summed, the four rules of addition can be satisfied. In Sec. V, we state our conclusion on the usefulness of coupled AB rings as computing circuits. Even though we investigated strictly one-dimensional ballistic quantum networks, it has been conjectured that, in much thicker AB rings, only a limited mode, which fits into the one-dimensional model, is dominant in the network, just like the situation in a classical waveguide. If this conjecture is true, an experimental realization of electron wave computing is possible. The current lithography-based microelectronic technology already exists today for this type of computing. In 1985, fabrication and

transport properties of a single AB ring with two terminals were demonstrated.[7] With minor modification, it is possible to insert a common center path, essentially halving the single AB ring and producing an equivalent irreducibly coupled AB ring network. Therefore, the tools to make this type of computing possible exist today and just need further development. The electron waveguide network is very similar to the corresponding superconducting network, as described by the de Gennes-Alexander theory.[16] However, the electron waveguide network is an easier extension in terms of construction from our current microelectronic technology.

II. BAND STRUCTURE AND PERSISTENT CURRENT IN ISOLATED AND IRREDUCIBLY COUPLED AB RINGS

In a strictly one-dimensional ballistic quantum network, nodes and path length bonds connect two adjacent nodes together. The electron wave function at any location in the network must satisfy the Schrödinger equation. Thus, an electron wave propagates along a given bond length and is scattered elastically at each node point. In addition, the phase of the electron wave function along a given path can be further modulated by the applied fluxes. The node equation approach reformulates the Schrödinger equation for the network by relating the electron wave functions at each node point with those at neighboring nodes.[10] For a given node at x (see Fig. 2) connected through a bond length l_{xy} to all the neighboring nodes at y, the resulting node equation for a plane wave along the network is from the Kirchhoff law such that the electron wave function at node x, $\Psi(x)$, satisfies

$$\left[\sum_y \cot(kl_{xy}) - iD\right]\Psi(x) - \sum_y \left[\csc(kl_{xy})\exp[i\phi l_{xy}]\Psi(y)\right] = 0, \tag{1}$$

where $k = \sqrt{2mE}/\hbar$ and E is the electron energy. ϕ is related to the applied flux Φ by $\phi = (2\pi/M)(\Phi/\Phi_0)$, where M is the total number of nodes in a loop (or ring). $D = (1 - R)/(1 + R)$, where R is the reflection amplitude if node x is an input terminal from y_1, y_2, or y_3, $D = -1$ if node x is an output terminal, and $D = 0$ if node x is simply internal by being neither an input nor an output terminal. Transmission probability, $T = 1 - |R|^2$, is then used in calculating the conductance in the Landauer-Büttiker formulation.[17–22]

Note that the bond lengths are in the unit of multiple atomic spacing ($l_{xy} = na$, for example). Thus, even or odd-numbered magnification also applies to the same network; that is, the n-factor can be magnified an even or odd number of times, satisfying a set of scaling rules.[12] Thus, it is sufficient to present small-scale toy models (the smallest n integer) when considering the band structures for each type of network.

If the flux modulation is set equal to zero, Eq. (1) is similar to coupled harmonic oscillators of the same topology with a mass located at each atom and spring constants associated with all neighboring atoms, as shown in Fig. 2. When two AB rings are irreducibly merged together, two situations can arise with respect to the common center path. Single and double-bonds capable of forming this path are shown and investigated. If the M3S and M3D cases (both shown in Fig. 1) are chosen to be examined for illustration purposes, where M3S labeling is for $M = 3$ atoms on a ring and S for single common center path when coupled, the generalized node equation approach from Eq. (1) for the four nodes, labeled as A, B, C, and D, reduces to

$$2\cos(ka)\Psi(A) - \exp[i\phi_1 a]\Psi(B) - \exp[-i\phi_1 a]\Psi(D) = 0, \tag{2}$$

$$n\cos(ka)\Psi(B) - \exp[-i\phi_1 a]\Psi(A) - \exp[i\phi_2 a]\Psi(C) - n'\exp[i(\phi_1 - \phi_2)a]\Psi(D) = 0, \tag{3}$$

$$2\cos(ka)\Psi(C) - \exp[i\phi_2 a]\Psi(D) - \exp[-i\phi_2 a]\Psi(B) = 0, \tag{4}$$

$$n\cos(ka)\Psi(D) - \exp[i\phi_1 a]\Psi(A) - \exp[-i\phi_2 a]\Psi(C) - n'\exp[i(\phi_2 - \phi_1)a]\Psi(B) = 0, \tag{5}$$

where $\Psi(A)$ is the electron wave function at node A and so on, $n = 3$, and $n' = 1$ for the single-bond case (M3S), while $n = 4$ and $n' = 2$ for the double-bond case (M3D). $\phi_1 = (2\pi/M_1)(\Phi/\Phi_0)$, where M_1 is the number of atoms on the left ring (3 in this case) and Φ_0 is the elementary flux quanta. Similarly, for ϕ_2, the relation to the applied flux for the right ring can be defined. We note that, if there is a potential associated with each node, then it can be shown that the $\cos(ka)$ factor in Eqs. (2)–(5) for the plane wave will be replaced with a form factor.[10] The resulting secular equation leads to the requirement for the electron energy E, with respect to the applied fluxes. In the general situation of an (l,m,n) configuration with spacing in units of atomic spacing a (see Fig. 3) for the left ring, right ring, and common center path, respectively, all the eigenenergies must satisfy the following equation for the single-bond case:

$$\begin{aligned} 3\sin(kl)\sin(km)\sin(kn) - 2\begin{bmatrix}\cos(kl)\cos(km)\sin(kn) + \\ \cos(km)\cos(kn)\sin(kl) + \\ \cos(kn)\cos(kl)\sin(km)\end{bmatrix} \\ + 2[\cos(l\phi_1 + m\phi_2)\sin(kn) + \cos(l\phi_1 + n\phi_3)\sin(km) \\ + \cos(m\phi_2 - n\phi_3)\sin(kl)] = 0, \end{aligned} \tag{6}$$

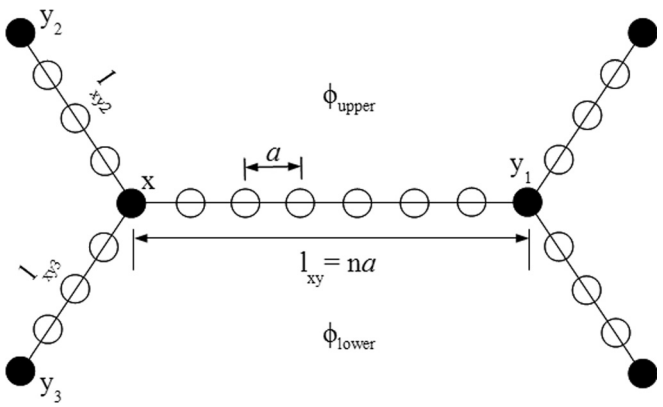

FIG. 2. Harmonic oscillator model—dots are masses; bond lengths are springs.

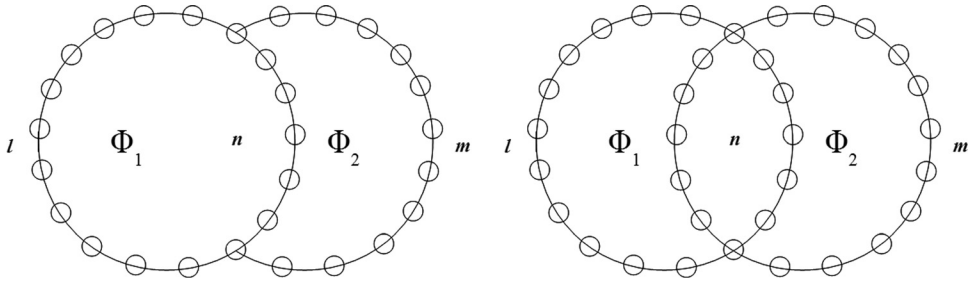

FIG. 3. The general (l,m,n) single-bond (left) and double-bond (right) configurations. In the M3S configuration of Fig. 1, $(l,m,n)=(2,2,1)$, while in the M4S configuration, $(l,m,n)=(3,3,1)$ and so on. Note that the transmission behavior for (6,6,3), (10,10,5), or (14,14,7) is preserved to that of (2,2,1).

where $\phi_3 = (\phi_1 - \phi_2)$. Similarly, the eigenenergies satisfy for the double-bond case:

$$3\sin(kl)\sin(km)\sin(kn) - \begin{bmatrix}\cos(kl)\cos(km)\sin(kn)+\\ 2\cos(km)\cos(kn)\sin(kl)+\\ 2\cos(kn)\cos(kl)\sin(km)\end{bmatrix} + [\cos(l\phi_1 + m\phi_2)\sin(kn) + 2\cos(l\phi_1 + n\phi_3)\sin(km) + 2\cos(m\phi_2 - n\phi_3)\sin(kl)] = 0. \quad (7)$$

Note that the flux periodicity is generally determined by the last three terms in Eqs. (6) or (7) when those cosine functions repeat. As an example, if we solve Eq. (6) where $(l,m,n)=(3,3,1)$ for the M4S case (shown in Fig. 1), Fig. 4 demonstrates the band structure and persistent current for such networks when $\Phi_1 = \pm\Phi_2 = \Phi$. Notice that, due to the strong coupling, there is a Fermi level crossover at $\Phi \approx \pm(^2/_9)\Phi_0$. This contributes to the discontinuity exhibited by the persistent current and designates a flux-enclosed anti-bonding region. There are six eigenstates and the Fermi level is located at the third-lowest level in a half-filled situation at temperature T = 0 K.

For any configuration of coupled AB rings, if all the bond lengths a are scaled up an odd number of times, $2n+1$, with n an integer, the Fermi level dependence on the flux remains the same, because the $\cos(ka)$ factor in every term is scaled up to become $\cos((2n+1)ka)$ and the persistent current is scaled down by the factor of $1/(2n+1)$, thus preserving transmission.

In an odd-even (M34) network, when two AB rings of different size are interacting with each other, this creates a complex problem. First, we note that each bond length must have the same fundamental unit: an integer unit of atomic spacing. Thus, two rings will have two different cross-sectional areas or two different total flux values for Φ_1 and Φ_2. For $M = 3$, it is denoted as Φ_{03}, and for $M = 4$, it is Φ_{04}. Therefore, $\Phi_{04} = (^{16}/_9)\Phi_{03}$. This extra factor will change the flux periodicity drastically, since the three cosine functions are now repeating at offset multiples from one another. Due to this, the flux periodicities for $M34S^+$, $M34D^+$, $M34S^-$, and $M34D^-$ are all given by a rather large $\Phi = 9\Phi_0$.

III. ELECTRON TRANSMISSION PROBABILITIES IN IRREDUCIBLY COUPLED AB RINGS HAVING THREE EXTERNAL TERMINALS

When three external terminals are to be attached to an M3 network (Fig. 1), one can arbitrarily pick three locations out of the four nodes (labeled as A, B, C, and D). Therefore, only four unique configurations of transmission exist. All others are the equivalent of the above four varieties by the argument from the Büttiker symmetry principle.[8] We will

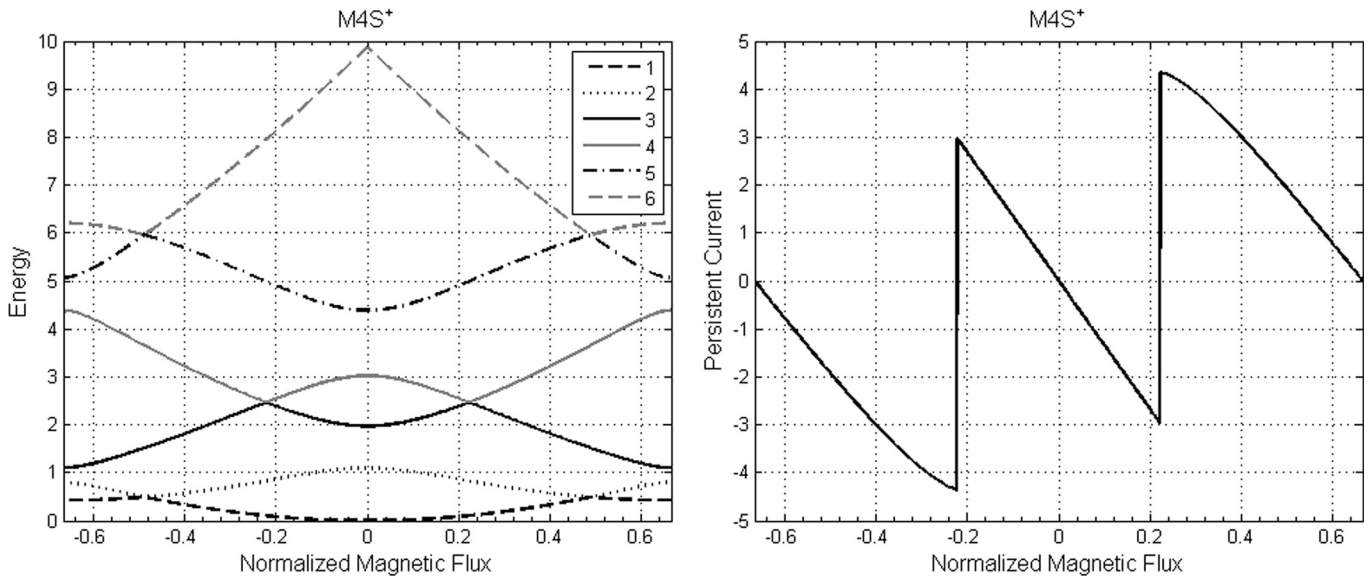

FIG. 4. Band structure (left) and persistent current (right) for $M4S^+$. Here, $M4S^+$ is for $M = 4$ atoms in each ring with a single-bond and applied fluxes $\Phi_1 = \Phi_2 = \Phi$.

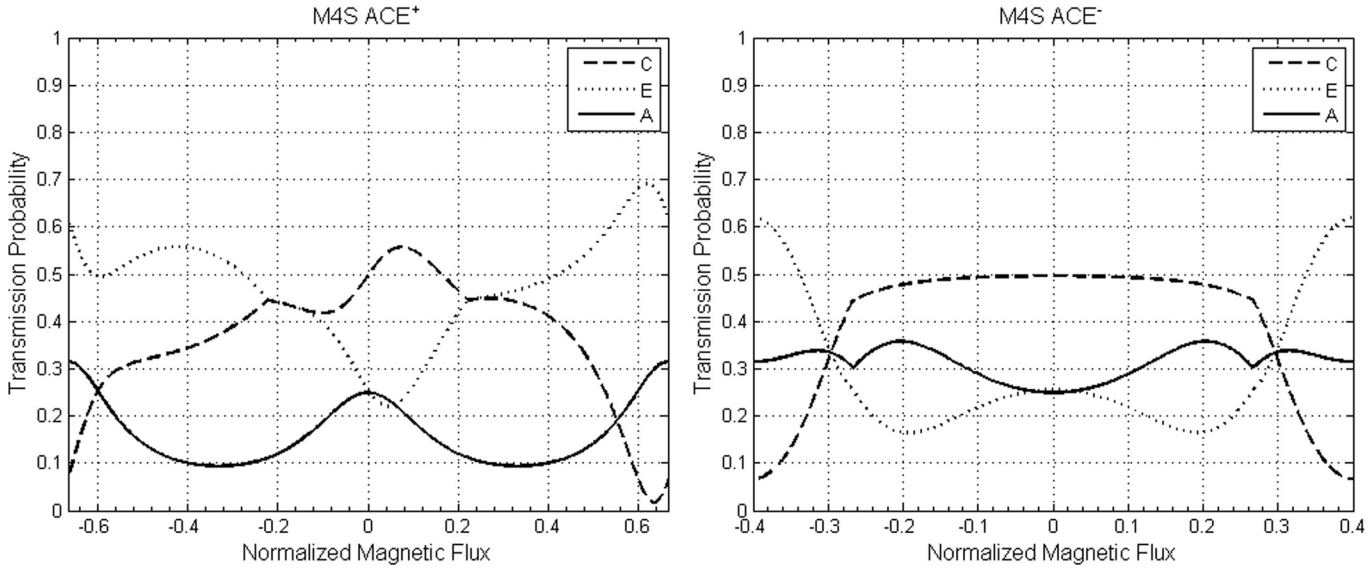

FIG. 5. Class (I) equivalently distributed network with M4S ACE$^+$ (left), M4S ACE$^-$ (right). All three terminals (A, C, E) share approximately a third of the transmission.

denote those configurations as ABD, ACD, DAC, and DBC. The ABD configuration here denotes the input is from terminal A and the outputs are going to terminals B and D.

With three terminals, the outputs are generally divided into three distinct classes. Class (I) can be described as when all terminals share the output with approximately a third transmission probability. We show one example of Class (I), by picking the M4S ACE network, in Fig. 5. Class (II) is when two terminals share the output roughly equally, while the third terminal has a diminished role. This is shown in Fig. 6 for the M4S FBD network. These first two classes are distributed output cases. Lastly, Class (III) describes when one terminal dominates the output at near total transmission probability, with the other two having diminished roles at that particular broad flux range. This is shown in Fig. 7 for the M4D ABF network. Thus, it is possible to state that electron transport for any of the six general network configurations (M3, M4, M34) having three external terminals must fall into one of the three classes just discussed. Thus, we expect an experimental realization will fall into one of the three classes. We note that, if one terminal dominates the share of the transmitted output (meaning Class (III) behavior), it is a desirable circuit for computing purposes that require only a single output to be high at once.

When two rings are of different size, as in the M34 case, there are 18 unique terminal configurations, more than the M4 case due to its anti-symmetric geometry. The transport behavior is more complex and spread over a larger flux range, as discussed in Sec. II. These properties make such network configurations less useful, in general, for constructing logic circuits.

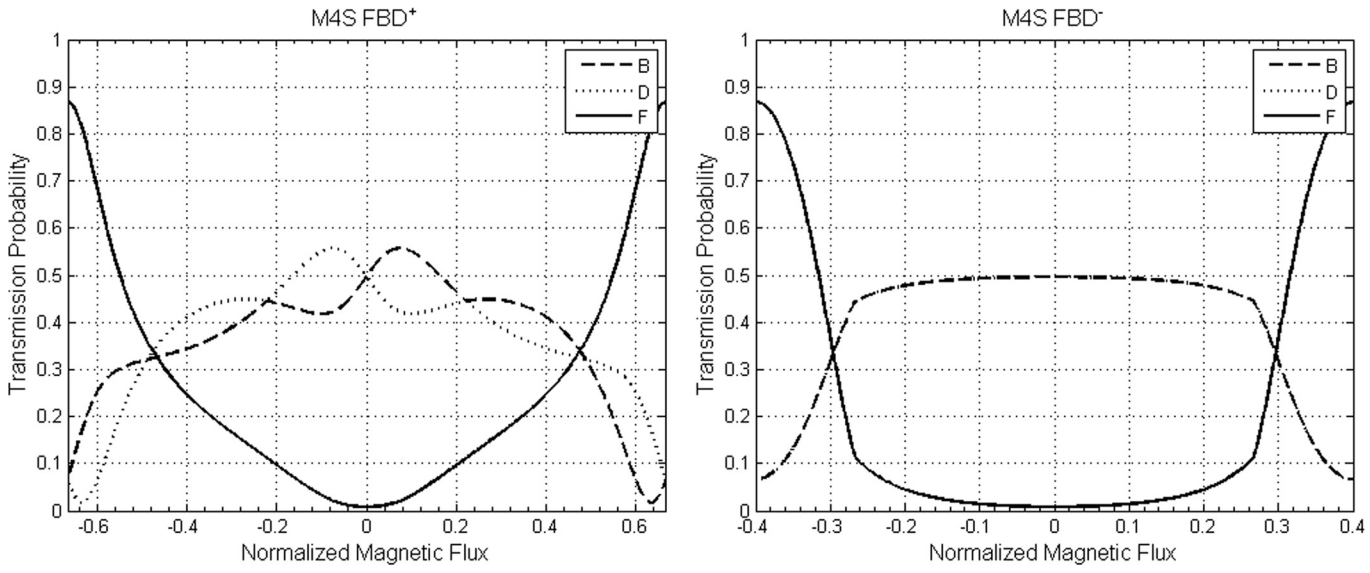

FIG. 6. Class (II) distributed network M4S FBD$^+$ (left), M4S FBD$^-$ (right). Terminals B and D share approximately half of the transmission, while F has a diminished role.

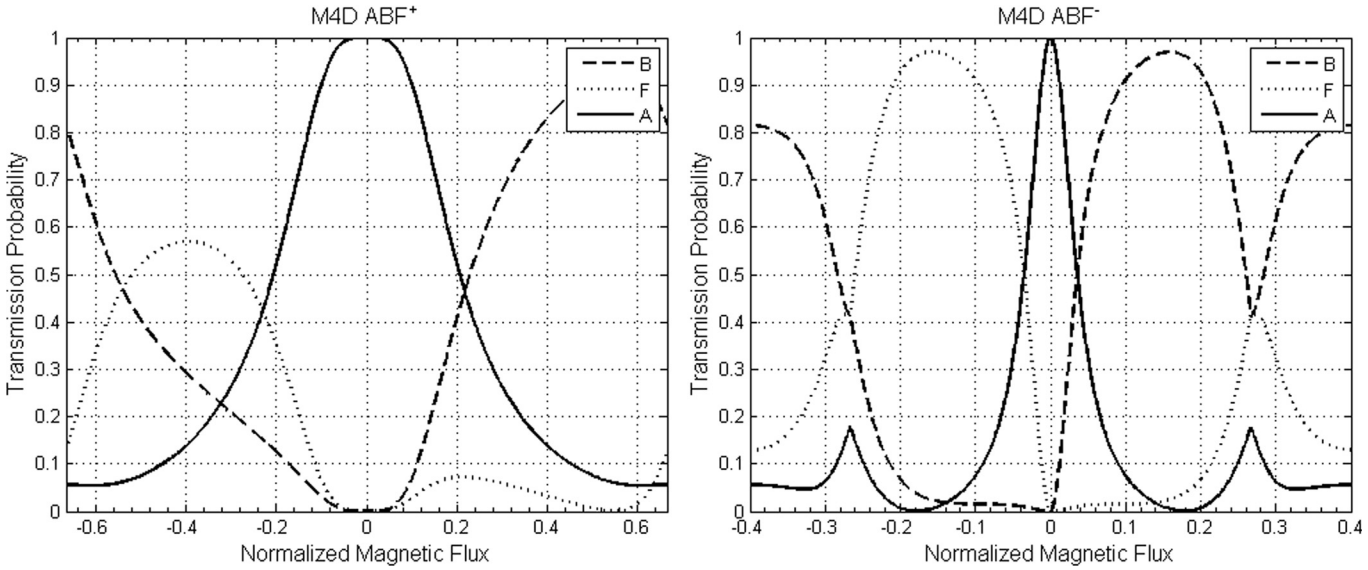

FIG. 7. Class (III) one terminal dominant network M4D ABF^{+} (left), M4D ABF^{-} (right). The domination occurs at different flux ranges for different terminals.

IV. APPLICATIONS OF IRREDUCIBLY COUPLED AB RINGS FOR COMPUTING: A HALF-ADDER EXAMPLE

By analyzing the electron transmission behavior of coupled AB rings, it is possible to realize them in such a way to be useful for performing digital logic operations. Due to favorable transmission relations for three-terminal networks, it is possible to produce functional non-unique operating models of many different traditional computing structures. From Class (III) transmission, one such possibility is the emulation of half-adder operation, which shares a two-input relationship with a coupled AB ring network. Organizing experimental transport results has allowed us to determine that, while several configuration possibilities exist, the M4D structure with terminal configuration ABF in Fig. 7 is the best Class (III) example to illustrate half-adder functionality. In this equivalent three-terminal case, depicted by Fig. 8, A is the applied current source to the network as well as the measured sum output, made possible by using a three-terminal quantum circulator at the node.[12] B is the carry out (cout), while F is the dump terminal, which provides a return path for the current to prevent unwanted transmissions at the sum and carry out terminals and ensures all possible logical combinations are satisfied.

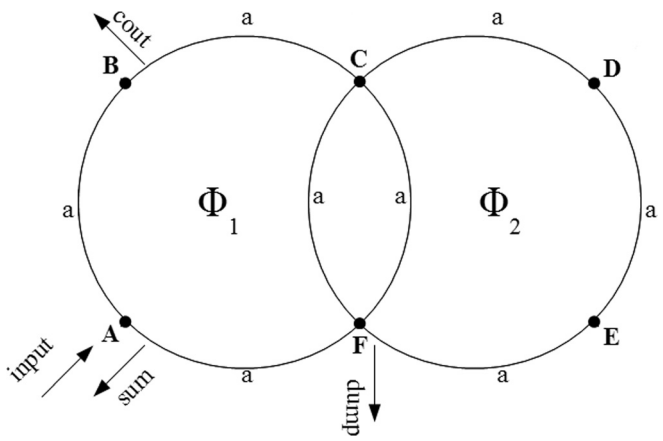

FIG. 8. Half-adder logic circuit represented by the M4D ABF network.

It is further necessary to establish the physical relationship between the network and logical inputs (1's and 0's), which need to be added. We note that, while the logical outputs are measureable currents, the inputs can instead be realized as the applied fluxes for each ring, Φ_1 and Φ_2. Similar to the spintronic inputs of spin-up (spin-down), a flux-mapping rule is developed in order to create the logical to physical connection. The simple rule implies that properly mapped fluxes must be of equal magnitude and can only differ by opposite sign, leading to four distinct possible input combinations (just like a half-adder): $\uparrow\downarrow$, $\uparrow\uparrow$, $\downarrow\downarrow$, $\downarrow\uparrow$. By setting when $\Phi_1 = \Phi_2 = \Phi$ and when $\Phi_1 = -\Phi_2 = \Phi$, it is possible to observe where these four combinations exhibit desirable transmission modes for half-adder operation in the network. For this, properly mapped fluxes must exhibit no incorrect transmissions under all four conditions across the flux period range and is the reason why a dump terminal, or discounted terminal, is necessary. In other words, three terminals are necessary for half-adder computing. In Fig. 9, adapted transmission plots (from Fig. 7) are shown for the network. Upon close examination, it can be noticed that, in the $\pm 0.1\Phi_0$ range, there is interesting transport phenomena. High transmission probabilities are observed for the appropriately chosen output terminals, ≈ 0.9, forcing unwanted transmissions at the other terminals to be very low, ≈ 0.1. Exploiting these results and connecting them with the spin-up (spin-down) principles, it is possible to extract the four distinct total combinations for half-adder operation. Basically, at a fixed flux value Φ, when $\Phi_1 = -\Phi_2 = \Phi$, the output at F is high and outputs at A (sum) and B (cout) are negligible. Thus, Rule I is satisfied, as shown in Table I and labeled on Fig. 9. The remaining three rules are presented in the same manner. For a half-adder, the general principle is to pick the appropriate high current output terminals for the

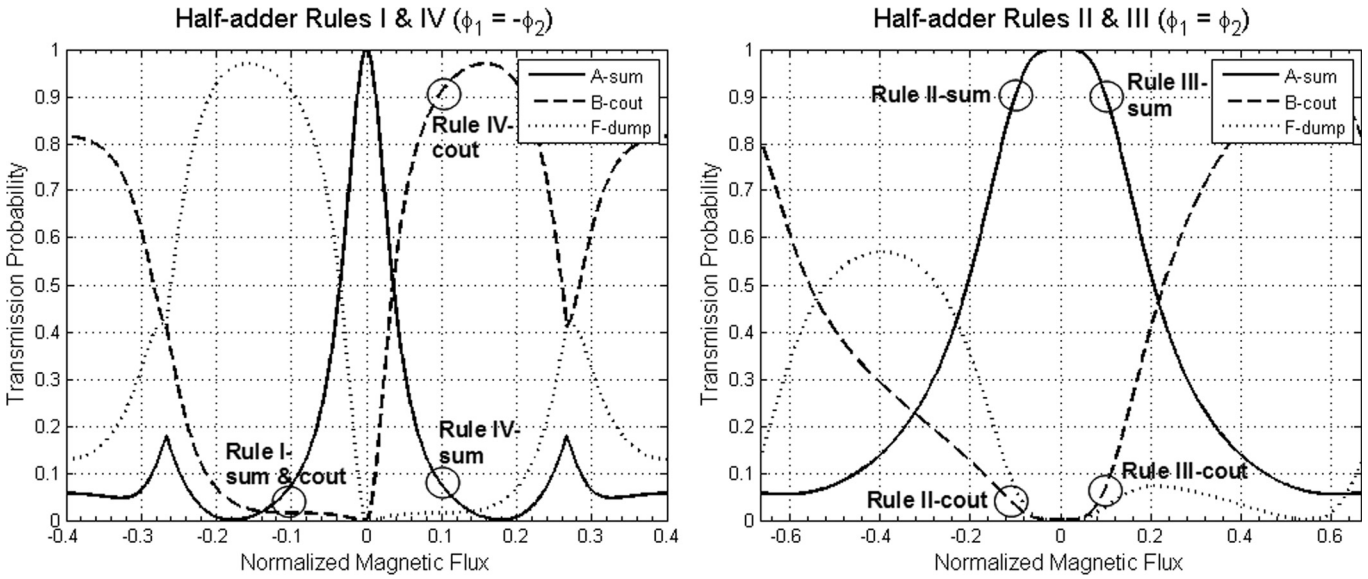

FIG. 9. Transmission results for the M4D ABF network when operating as a half-adder.

sum and carry out, thus allowing the four flux directional combinations to be mapped into the four configurations of addition.

By utilizing the concept of inputs being introduced into irreducibly coupled AB ring networks as applied directional fluxes (spintronic inputs), while outputs are measurable currents, it is possible to extend the functionality of coupled AB rings to be used for a whole host of other digital logic device families. The key is finding the appropriate class of the coupled AB ring structure, such as Class (III) transmission, and its corresponding terminal arrangements, which exhibit the correct flux-mapping relationships for the specific logical operations necessary for operation. This points out the need to establish the fundamental mode of propagation associated with a given AB ring dimension and the terminal locations that can transmit an input near totally to a proper output terminal symmetrically and anti-symmetrically with respect to the change of flux sign. We believe this strongly demonstrates a new way of thinking about physically structuring next-generation computing architecture — by using coupled AB ring network topologies, where properly chosen applied fluxes can act as logical input bits to induce modulated transmission modes via the AB effect for digital logic operations.

V. CONCLUSION

Electron transmission through two irreducibly coupled Aharonov-Bohm rings via multi-terminals is modeled as flux-assisted coupled harmonic oscillators of the same topology. The three-terminal cases shown here are of particular interest. The transmission depends strongly on the number of atoms in each ring as well as on the terminal locations. All six general configurations have been discussed. The flux periodicity is determined from a two-dimensional Brillouin zone due to the fact that there are two modulating fluxes present, and this value is generally a rational number of the elementary flux quanta. The general equations for determining the flux periodicity for two single and double-bonded coupled AB rings are provided here. We present the transmission results when the two fluxes are of the same direction and of opposite direction, corresponding to two different spins or the circulating persistent current directions in each ring. The transmission probability can be classified into three distinctive behaviors: The first class is for an input to be more or less equally distributed to all three output terminals in a broad flux range. The second class is for two terminals to share roughly half of the transmission each, while the third

TABLE I. Rules for the M4D ABF half-adder flux-mapping relationships (see Fig. 9).

Half-adder rule	Input bits to add	Flux mapping (Φ_1,Φ_2)	Logical outputs at terminals	Satisfied at (Φ_1,Φ_2)	Transmission results
I	0 0	($\uparrow$, $\downarrow$)	A (sum) = 0	(−0.1, +0.1) Φ_0	$T_A = 0.1$
			B (cout) = 0		$T_B = 0.1$
II	0 1	($\uparrow$, $\uparrow$)	A (sum) = 1	(−0.1, −0.1) Φ_0	$T_A = 0.9$
			B (cout) = 0		$T_B = 0.1$
III	1 0	($\downarrow$, $\downarrow$)	A (sum) = 1	(+0.1, +0.1) Φ_0	$T_A = 0.9$
			B (cout) = 0		$T_B = 0.1$
IV	1 1	($\downarrow$, $\uparrow$)	A (sum) = 0	(+0.1, −0.1) Φ_0	$T_A = 0.1$
			B (cout) = 1		$T_B = 0.9$

terminal is more or less bypassed. The third and final class is for one terminal to dominate the transmission at near unity, while the other two terminals are bypassed at a broad flux range. When two AB rings of different size are interacting with each other, such as from the odd-even combined AB rings, the flux periodicity is greatly increased due to the cross-sectional area ratio, and the transmission behavior becomes very irregular and complex. Broadly speaking, the transmissions are divided into several fundamental modes similar to classical microwave transmission, except the classification scheme is determined by how even or odd-numbered AB rings are combined and by the locations of the terminals. Once those parameters are fixed, a scaled-up version of the same topology will preserve the same transmission behavior if the magnification factor is by an odd number of times. We present the smallest possible configurations in this paper and expect, experimentally, that the transmissions must fall automatically into one of the three classes discussed, regardless of the size or geometry, as long as a coupled AB ring structure with three terminals is preserved.

Because of the four different spin pairings from the two possible directions of the circulating persistent currents in each AB ring, one can map each pairing configuration into one of the four rules of binary addition when two digits are being added. The flux directions are then used as the inputs for the two digits. The outputs for the sum and carry out require two external terminals, which we have identified properly by an example where the transmissions can indeed be dominated by one particular terminal (the Class (III) transmission) to satisfy all four half-adder rules evaluated at one particular value (at a board range) of the applied fluxes simultaneously. This is made possible by observing the symmetric (for the sum terminal) and anti-symmetric (for the carry out terminal) properties of the transmissions with respect to the change of the flux sign. Thus, for a full-adder, one can expect to use three irreducibly coupled AB rings with three flux directions as the inputs to satisfy the eight rules of a full-adder, in principle. A higher number of coupled AB rings can thus be expected to perform higher-order computations. These kinds of quantum circuits can be realized experimentally if there is only one fundamental mode dominating the propagation in the electron waveguide of a thicker cross section. By utilizing existing technology for a single AB ring with two terminals,[7] if a third terminal is added and center common path inserted, thus halving the ring, the resulting irreducibly coupled AB ring network makes it possible to realize this form of electron wave computing. At first glance, it may appear that our quantum computing method relies on very complicated phase coherent electron interference. However, we want to emphasize that the transmission behavior for any three-terminal construction of two irreducible AB rings will result in one of the three classes discussed here, with one being useful for quantum computing circuits.

ACKNOWLEDGMENTS

We would like to thank Mr. Lee Tran for his Master's thesis work in the calculations of the charge accumulation profiles along the center common path in the models as the flux values are varied.

[1]A. Tonomura, N. Osakabe, T. Matsuda, T. Kawasaki, and J. Endo, Phys. Rev. Lett. **56**, 792 (1986).
[2]S. Washburn and R. A. Webb, Adv. Phys. **35**, 375 (1986).
[3]H. Ajiki and T. Ando, Physica B **201**, 349 (1994).
[4]A. Tonomura, Proc. Jpn. Acad., Ser. B **82**, 45 (2006).
[5]R. Jackiw, A. I. Milstein, S. Y. Pi, and I. S. Terekhov, Phys. Rev. B **80**, 033413 (2009).
[6]X. C. Xie and S. Das Sarma, Phys. Rev. B **36**, 9326 (1987).
[7]R. A. Webb, S. Washburn, C. P. Umbach, and R. B. Laibowitz, Phys. Rev. Lett. **54**, 2696 (1985).
[8]M. Büttiker, IBM J. Res. Dev. **32**(3), 317 (1988).
[9]D. Awschalom, M. Flatte, and N. Samarth, Sci. Am., **286**(6), 66 (2002).
[10]C. H. Wu and G. Mahler, Phys. Rev. B **43**, 5012 (1991).
[11]T. Chwiej and B. Szafran, Phys. Rev. B **78**, 245306 (2008).
[12]C. H. Wu and D. Ramamurthy, Phys. Rev. B **65**, 075313 (2002).
[13]C. H. Wu and D. Ramamurthy, Phys. Rev. B **66**, 115307 (2002).
[14]L. Tran, M.S. thesis, Missouri University of Science and Technology, 2006.
[15]T. Hatano, T. Kubo, Y. Tokura, S. Amaha, S. Teraoka, and S. Tarucha, Phys. Rev. Lett. **106**, 076801 (2011).
[16]S. Alexander, Phys. Rev. B **27**, 1541 (1983).
[17]R. Landauer, Philos. Mag. **21**, 863 (1970).
[18]R. Landauer and M. Büttiker, Phys. Rev. Lett. **54**, 2049 (1985).
[19]M. Büttiker, Y. Imry, and R. Landauer, Phys. Lett. **96A**, 365 (1983).
[20]M. Büttiker, Y. Imry, and M. Azbel, Phys. Rev. A **30**, 1982 (1984).
[21]M. Büttiker, Y. Imry, R. Landauer, and S. Pinhas, Phys. Rev. B **31**, 6207 (1985).
[22]P. W. Anderson, D. J. Thouless, E. Abrahams, and D. S. Fischer, Phys. Rev. B **22**, 3519 (1980).